



Supporting Information

Unusual Reactivity of *cyclo*-(P₅Ph₅): Oxidative Addition at a Group 6 Metal Carbonyl and Insertion of Acetonitrile into a P–P Bond

Divine Mbom Yufanyi, Toni Grell, and Evamarie Hey-Hawkins*

[ejic201900027-sup-0001-SupMat.pdf](#)

Table of Contents

Item	Description	Page
Experimental Procedures	Synthesis of the complexes	2
Data Collection and Structure Refinement		3
Results and Discussion		3
Figure S1	Molecular structure and atom-labelling scheme for 1a with ellipsoids drawn at 50% probability level. H atoms are omitted for clarity.	3
Figure S2	Molecular structure and atom-labelling scheme for 1b with ellipsoids drawn at 50% probability level. H atoms are omitted for clarity.	4
Figure S3	Molecular structure and atom-labelling scheme for 2 (Mo/W disordered, only one distribution is shown) with ellipsoids drawn at 50% probability level. H atoms are omitted for clarity.	4
Table S1	Crystallographic data for complexes 1a–c , 2c and 2	4
Table S2	Selected bond lengths (Å) and angles (°) for 1a–c , 2c and 2 .	5
Scheme S1	This mechanism for the formation of 1a–c does not involve an oxidative insertion and is thus unlikely.	5
Scheme S2	This mechanism for the formation of 1a–c leads to the wrong constitutional isomer and thus is ruled out.	6
Table S3	³¹ P{ ¹ H} NMR data (δ (ppm) and J (Hz)) of compounds 3a–c in C ₆ D ₆ at 25°C	7
Figure S4	Experimental (top) and simulated (bottom) ³¹ P{ ¹ H} NMR spectrum of complex 1a in C ₆ D ₆ .	8
Figure S5	Experimental (top) and simulated (bottom) ³¹ P{ ¹ H} NMR spectrum of complex 1b in C ₆ D ₆ .	8
Figure S6	Experimental (top) and simulated (bottom) ³¹ P{ ¹ H} NMR spectrum of complex 1c in C ₆ D ₆ .	9
Figure S7	³¹ P{ ¹ H} NMR spectrum of complex 2c in C ₆ D ₆ .	9
Figure S8	Time-dependent experimental ³¹ P{ ¹ H} NMR spectra for the formation of complex 2c compared to that of 1c in C ₆ D ₆ .	10
Table S4	CO and C=N vibrations (cm ⁻¹) of compounds 1a–c and 2c .	10
Figure S9	IR spectra of complexes compounds 1a–c and 2c .	11
Figure S10	TG/DTA/MS plots for 1b (left) and 1c (right).	12
Table S5	Thermal decomposition data of 1b and 1c up to 900 °C.	12
Figure S11	Powder XRD patterns of the thermal decomposition products of 1b (left) and 1c (right).	12
References		13

Experimental Procedures

General Remarks

All experiments were performed under an atmosphere of dry nitrogen using standard Schlenk techniques. Solvents were dried and freshly distilled under nitrogen and kept over molecular sieve 4 Å. The NMR spectra were recorded at 25 °C with a Bruker AVANCE DRX 400 spectrometer (¹H NMR: 400.13 MHz, ³¹P NMR: 161.97 MHz). TMS was used as internal standard for ¹H NMR spectra. ³¹P NMR: 85% H₃PO₄ was used as external standard. The chemical shifts and coupling constants were obtained with the simulation program SpinWorks 4.^[1] Mass spectrometry measurements were carried out as ESI-MS with a BRUKER Daltonics FT-ICR-MS spectrometer (Type APEX II, 7 Tesla). IR spectra: KBr pellets were prepared in a nitrogen-filled glove box and the spectra were recorded on a PerkinElmer System 2000 FTIR spectrometer in the range 350-4000 cm⁻¹. Elemental analyses for C, H, and N were performed on a FlashEA1112 element analyser. In some cases, formation of carbides can result in a lower carbon content. Thermogravimetric (TG) and differential thermal analysis (DTA) curves, coupled with mass spectrometry, were obtained using a NETZSCH STA449F1 thermoanalyser in a dynamic argon atmosphere (heating rate 10 °C·min⁻¹, flow rate 25 mL·min⁻¹, aluminium oxide crucible, mass 20 mg, and temperature range from room temperature up to 900 °C).

Materials

[Cr(CO)_y(MeCN)_x] (x = 1, y = 5; x = 2, y = 4), [Mo(CO)₄(nbd)] (nbd = 2,5-norbornadiene),^[2] [W(CO)₄(MeCN)₂],^[3] and *cyclo*-(P₅Ph₅)^[4] were synthesised according to literature methods. *Cyclo*-(P₅Ph₅) (**1**) was recrystallised from hot toluene to obtain crystals of higher purity and quality. Compounds **1a-c** were synthesised as previously reported.^[5]

Synthesis of the Complexes

Synthesis of **1a**

At room temperature, a solution of [Cr(CO)₄(MeCN)₂] (0.276 g, 1.12 mmol) in toluene (20 mL) was added dropwise to a solution of *cyclo*-(P₅Ph₅) (0.36 g, 0.56 mmol) in toluene (20 mL). The colour of the solution changed from cream white through orange to brown during the addition. The reaction mixture was stirred at room temperature for 30 minutes and then refluxed overnight at 120 °C to give a reddish-brown mixture. The solvent was removed *in vacuo* and the resulting black solid was re-dissolved in CH₂Cl₂. Slow diffusion of Et₂O into this solution at 0 °C afforded **1a** as black crystals (387.9 mg, 68.2%): ¹H NMR (C₆D₆): δ = 8.2-6.6 (m, Ph); ³¹P{¹H} NMR (C₆D₆): see Table S3; IR (KBr): $\tilde{\nu}$ = 1991 (s), 1953 (vs), 1938 (vs), 1906 (sh), 1880 cm⁻¹ (sh) (CO); elemental anal. calcd (%) for C₃₈H₂₈Cr₂NO₆P₅ (853.46): C 53.48, H 3.31, N 1.64; found: C 52.13, H 3.14, N 1.52.

Synthesis of **1b**

At room temperature, a solution of [Mo(CO)₄(nbd)] (0.24 g, 0.74 mmol) in toluene (15 mL) was added dropwise to a solution of *cyclo*-(P₅Ph₅) (0.21 g, 0.37 mmol) in toluene (15 mL). 5 mL of MeCN were added to this solution. The color of the solution changed from cream white through orange to brown during the addition. The reaction mixture was stirred at room temperature for 30 minutes and then refluxed overnight at 120 °C to give a dark-brown mixture. The solvent was removed *in vacuo* and the resulting black solid was re-dissolved in CH₂Cl₂. Slow diffusion of *n*-hexane into this solution at 0 °C afforded **1b** as black crystals (353.1 mg, 96.5%): ¹H NMR (C₆D₆): δ = 8.2-6.6 (m, Ph); ³¹P{¹H} NMR (C₆D₆): see Table S3; IR (KBr): $\tilde{\nu}$ = 2009 (s), 1969 (vs), 1954 (vs), 1920 (sh), 1890 cm⁻¹ (sh) (CO); elemental anal. calcd (%) for C₃₈H₂₈Mo₂NO₆P₅ (941.34): C 48.48, H 3.00, N 1.49; found: C 47.95, H 2.90, N 1.41.

Synthesis of **1c**

At room temperature, a solution of [W(CO)₄(MeCN)₂] (0.28 g, 0.74 mmol) in toluene (15 mL) was added dropwise to a solution of *cyclo*-(P₅Ph₅) (0.21 g, 0.37 mmol) in toluene (15 mL). The color of the solution changed from cream white through orange to brown during the addition. The reaction mixture was stirred at room temperature for 30 minutes and then refluxed overnight at 120 °C to give a reddish-brown mixture. The solvent was removed *in vacuo* and the resulting black solid was re-dissolved in CH₂Cl₂. Slow diffusion of *n*-hexane into this solution at 0 °C afforded **1c** as greenish-black crystals (311.1 mg, 71.7%): ¹H NMR (C₆D₆): δ = 8.2-6.6 (m, Ph); ³¹P{¹H} NMR (C₆D₆): see Table S3; IR (KBr): $\tilde{\nu}$ = 2074(w), 2005 (s), 1964 (vs), 1947 (vs), 1913 (sh), 1881 cm⁻¹ (sh) (CO), 1581 (w) cm⁻¹ (C=N); elemental anal. calcd (%) for C₃₈H₂₈NO₆P₅W₂ (1117.16): C 40.85, H 2.53, N 1.25; found: C 41.90, H 2.41, N 1.20.

The mass spectra of compounds **1a-c** in MeCN showed the molecular ion peak [M]⁺ at *m/z* 853.46, 941.34 and 1117.97, respectively.

Synthesis of 2c

At room temperature, a solution of *cyclo*-(P₅Ph₅) (0.162 g; 0.3 mmol) in toluene (15 mL) was added dropwise to a solution of [W(CO)₄(MeCN)₂] (0.378 g, 1 mmol) in toluene (20 mL). The reaction mixture was stirred at room temperature for 30 minutes and then refluxed at 120 °C for 48 h to give a dark-brown mixture. The color of the reaction medium changed from pale-yellow to orange to red-brown and finally dark-brown. The solvent was reduced *in vacuo* to 8 mL and filtered. The mixture of **1c** and **2c** was separated by chromatography on SiO₂, eluting with CH₂Cl₂. Slow diffusion of *n*-hexane into the CH₂Cl₂ solution of fraction 1 at 0 °C afforded **2c** as greenish-black crystals (397.7 mg, 27.6%): ¹H NMR (C₆D₆): δ = 8.6-6.4 (m, Ph); ³¹P{¹H} NMR (C₆D₆): see Table S3; IR (KBr): $\tilde{\nu}$ = 2073 (s), 2005 (s), 1976 (vs), 1940 (vs), 1923 (vs) cm⁻¹ (CO), 1632 (w) cm⁻¹ (C=N); Elemental anal. calcd (%) for C₄₃H₂₈NO₁₁P₅W₃ (1441.06): C 35.84, H 1.96, N 0.97; found: C 36.33, H 2.09, N 0.89.

In order to improve the synthesis of **2c**, [W(CO)₄(MeCN)₂] and *cyclo*-(P₅Ph₅) (ratio 3:1) were refluxed in toluene at 120 °C for 24 h and 48 h and in each case ³¹P{¹H} NMR spectra showed that a mixture of **1c** and **2c** was obtained (Fig. S8). This mixture was separated by column chromatography. A ³¹P{¹H} NMR analysis of the reaction mixture left in air overnight showed no change. Using a ratio of 3.5:1 and refluxing for 48 hours gave a mixture of **1c** and **2c** (according to ³¹P{¹H} NMR analysis).

Synthesis of 2

Refluxing [W(CO)₄(MeCN)₂] and **1b** in a 1:1 ratio resulted in a complex **2**, which is isostructural with **2c**. An independent mixed occupancy was applied for every metal site in the model, which led to improved *R* values for the structure model of this complex. The refinement yielded the following occupancies for the metal sites:

M1: 60.703% W 39.297% Mo

M2: 55.116% W 44.887% Mo

M3: 90.569% W 09.431% Mo

A mixed Mo/W complex [M(μ-PMe₂)(CO)₃(PMe₃)₂] (M = Mo and W in 1/4 ratio)^[10] is also known.

Data Collection and Structure Refinement

X-ray data were collected with a GEMINI CCD diffractometer (Rigaku Inc.), λ(Mo-K_α) = 0.71073 Å, *T* = 130(2) K, empirical absorption corrections with SCALE3 ABSPACK.^[6] All structures were solved by dual space methods with SIR-92.^[7] Structure refinement was done with SHELXL-2016^[8] by using full-matrix least-square routines against *F*². All hydrogen atoms were calculated on idealised positions. The pictures were generated with the program Mercury.^[9] CCDC 1888485 (**1a**), CCDC 1888484 (**1b**), CCDC 1888482 (**1c**), CCDC 1888486 (**2**, Mo/W disordered) and CCDC 1888488 (**2c**) contain the supplementary crystallographic data for this paper. These data can be obtained free of charge via www.ccdc.cam.ac.uk/data_request/cif (or from the Cambridge Crystallographic Data Centre, 12 Union Road, Cambridge CB2 1EZ, UK; fax: (+44)1223-336-033; or deposit@ccdc.cam.ac.uk).

Results and Discussion

The structures of the complexes **1a-c** and **2c** are presented in Figs. S1-S3 and the crystallographic data summarised in Table S1. Selected bond lengths are presented in Table S2.

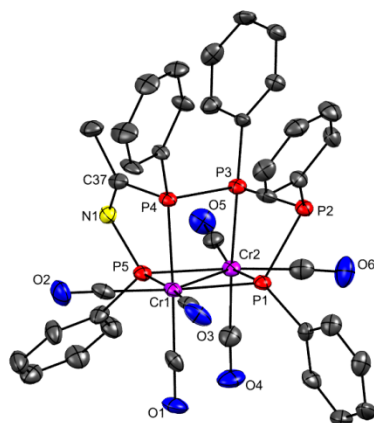


Figure S1. Molecular structure and atom-labelling scheme for **1a** with ellipsoids drawn at 50% probability level. H atoms are omitted for clarity.

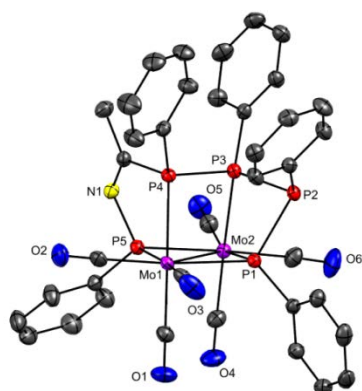


Figure S2. Molecular structure and atom-labelling scheme for **1b** with ellipsoids drawn at 50% probability level. H atoms are omitted for clarity.

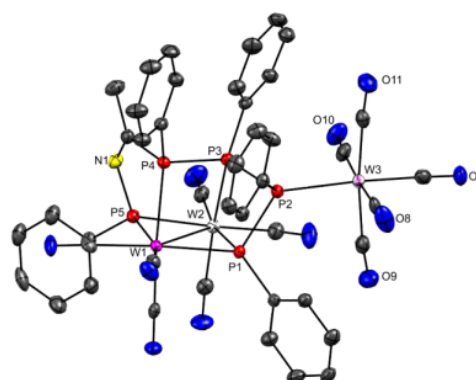


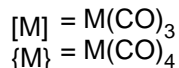
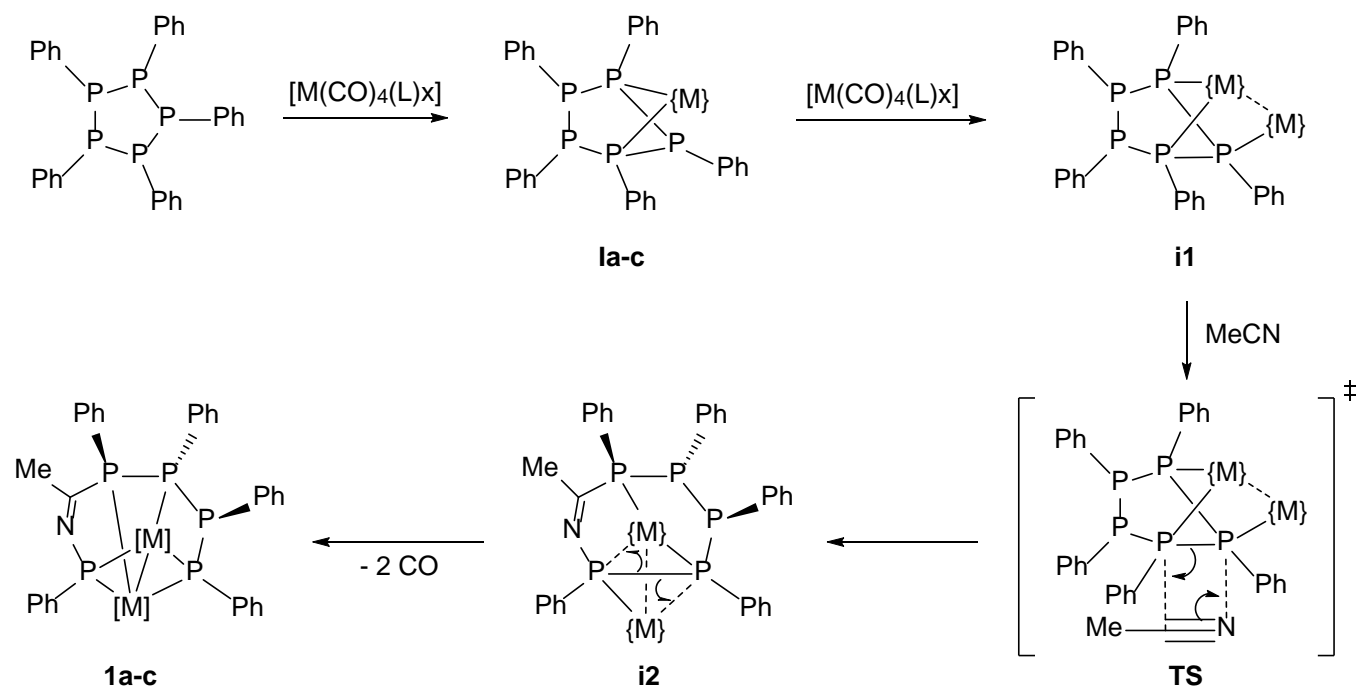
Figure S3. Molecular structure and atom-labelling scheme for **2** (Mo/W disordered, only the distribution with solely tungsten is shown) with ellipsoids drawn at 50% probability level. H atoms are omitted for clarity.

Table S1. Crystallographic data for complexes **1a–c** and **2c**, and **2**.

	1a	1b	1c	2c	2
Chemical formula	C ₃₈ H ₂₈ Cr ₂ NO ₆ P ₅	C ₃₈ H ₂₈ Mo ₂ NO ₆ P ₅	C ₃₈ H ₂₈ NO ₆ P ₅ W ₂	C ₄₃ H ₂₈ NO ₁₁ P ₅ W ₃	C ₄₃ H ₂₈ Mo _{0.94} NO ₁₁ P ₅ W _{2.06}
<i>M</i>	853.46	941.34	1117.16	1441.06	1358.76
Crystal system, space group	Triclinic, <i>P</i> $\bar{1}$	Triclinic, <i>P</i> $\bar{1}$	Triclinic, <i>P</i> $\bar{1}$	Monoclinic, <i>P</i> ₂ / <i>n</i>	Monoclinic, <i>P</i> ₂ / <i>n</i>
Temperature (K)	130	130	130	130	130
<i>a</i> , <i>b</i> , <i>c</i> (Å)	9.762(6), 11.432(5), 17.325(1)	9.799(1), 11.495(2), 17.575(3)	9.8152(3), 11.4914(3), 17.537(5)	12.398(2), 24.739(4), 14.869(2)	12.399(2), 24.779(3), 14.873(2)
α , β , γ (°)	87.26(5), 86.91(5), 71.25(5)	86.67(1), 87.98(1), 71.85(1)	86.59(2), 87.75(2), 71.745(3)	97.46(2)	97.48(1)
<i>V</i> (Å ³)	1827.38(2)	1877.67(5)	1874.65(1)	4522.00(1)	4530.69(1)
<i>Z</i>	2	2	2	4	4
Radiation type	Mo-K α	Mo-K α	Mo-K α	Mo-K α	Mo-K α
μ (mm ⁻¹)	0.86	0.93	6.39	7.85	5.72
Crystal size (mm)	0.07 × 0.05 × 0.05	0.2 × 0.2 × 0.1	0.1 × 0.03 × 0.03	0.1 × 0.1 × 0.08	0.08 × 0.04 × 0.02
<i>T</i> _{min} , <i>T</i> _{max}	0.978, 1	0.977, 1	0.763, 1	0.644, 1	0.922, 1
No. of measured, independent and observed [<i>I</i> > 2 σ (<i>I</i>)] reflections	12544, 6634, 3722	57840, 11464, 9736	37548, 11438, 9085	38747, 14794, 12747	50289, 15068, 11427
<i>R</i> _{int}	0.074	0.036	0.048	0.028	0.060
(<i>sin</i> θ / λ) _{max} (Å ⁻¹)	0.602	0.714	0.714	0.755	0.754
<i>R</i> [[<i>F</i> ² > 2 σ (<i>F</i> ²)], <i>wR</i> (<i>F</i> ²), <i>S</i>	0.067, 0.137, 1.00	0.029, 0.065, 1.07	0.031, 0.057, 1.02	0.028, 0.057, 1.09	0.040, 0.060, 1.01
No. of reflections	6634	11464	11438	14794	15068
No. of parameters	470	470	470	569	572
No. of restraints	0	0	0	0	0
H atom treatment	H atom parameters constrained	H atom parameters constrained	H atom parameters constrained	H atom parameters constrained	H atom parameters constrained
$\Delta\rho$ _{max} , $\Delta\rho$ _{min} (e Å ⁻³)	1.07, -0.53	0.60, -0.51	1.26, -1.23	1.75, -1.5	1.50, -1.34

Table S2. Selected bond lengths (Å) and angles (°) for **1a-c** and **2c**.

Bond Length (Å); Bond Angle (°)	1a (M = Cr)	1b (M = Mo)	1c (M = W)	2c (M = W)
M(1)–M(2)	2.893(1)	3.0253(2)	3.0279(2)	3.0279(2)
P(1)–M(1)	2.315(2)	2.4538(5)	2.454(1)	2.4948(8)
P(1)–M(2)	2.337(2)	2.4668(5)	2.4675(9)	2.4758(8)
P(2)–M(3)				2.5274(8)
P(3)–M(2)	2.387(2)	2.5161(5)	2.5091(9)	2.5161(8)
P(4)–M(1)	2.323(2)	2.4688(5)	2.4629(9)	2.4986(8)
P(5)–M(1)	2.297(2)	2.4335(5)	2.4363(9)	2.4361(8)
P(5)–M(2)	2.303(2)	2.4412(5)	2.442(1)	2.4349(9)
P(1)–P(2)	2.204(2)	2.2028(7)	2.205(1)	2.210(1)
P(2)–P(3)	2.192(2)	2.2008(7)	2.202(1)	2.245(1)
P(3)–P(4)	2.219(2)	2.2245(6)	2.230(1)	2.224(1)
P(5)–N(1)	1.748(5)	1.743(2)	1.743(3)	1.719(3)
C(37)–P(4)	1.859(6)	1.880(2)	1.883(4)	1.889(3)
C(37)–N(1)	1.280(6)	1.276(2)	1.274(4)	1.266(4)
M(1)–P(1)–M(2)	76.90(6)	75.88(2)	75.94(3)	75.06(2)
M(1)–P(5)–M(2)	77.95(6)	76.72(2)	76.72(3)	76.87(2)
P(2)–P(3)–P(4)	105.1(1)	106.29(3)	106.22(5)	103.09(4)
P(3)–P(2)–P(1)	77.69(7)	80.22(2)	79.76(5)	80.34(4)
P(5)–M(1)–P(1)	102.98(7)	103.86(2)	103.81(3)	103.61(3)
P(5)–M(2)–P(1)	102.12(7)	103.24(2)	103.22(3)	104.22(3)
C(37)–N(1)–P(5)	115.7(4)	118.3(2)	118.3(3)	119.3(2)



- a: M = Cr, L = MeCN, x = 2
 b: M = Mo, L = nbd, x = 1
 c: M = W, L = MeCN, x = 2

Scheme S1. This mechanism for the formation of **1a-c** does not involve an oxidative insertion and is thus unlikely.

Table S3. $^{31}\text{P}\{^1\text{H}\}$ NMR data (δ (ppm) and J (Hz), standard deviations in brackets) of compounds **1a-c** in C_6D_6 at 25°C . Numbering scheme is given in scheme 1.

	1a	1b	1c	2c
Chemical Shift (ppm)				
$\delta(\text{P}_\text{A})$	343.09(1)	305.12(1)	260.10(1)	260.57(1)
$\delta(\text{P}_\text{B})$	195.55(1)	145.56(1)	138.79(1)	116.97(1)
$\delta(\text{P}_\text{C})$	162.80(1)	141.20(1)	96.92(1)	115.75(1)
$\delta(\text{P}_\text{D})$	79.62(1)	62.07(1)	54.77(1)	90.28(1)
$\delta(\text{P}_\text{E})$	7.27(1)	19.09(1)	24.27(1)	60.53(1)
$J_{\text{P-P}}$ (Hz) and $J_{\text{W-P}}$ (Hz)				
$^2J(\text{P}_\text{A},\text{P}_\text{B})$	1.49(8)	10.21(3)	13.35(1)	
$^2J(\text{P}_\text{A},\text{P}_\text{C})$	89.69(7)	87.66(3)	103.05(1)	
$^2J(\text{P}_\text{A},\text{P}_\text{D})$	-0.00(7)	-0.00(3)	-0.03(9)	
$^2J(\text{P}_\text{A},\text{P}_\text{E})$	20.06(7)	14.65(5)	14.10(1)	
$^2J(\text{P}_\text{B},\text{P}_\text{C})$	10.99(8)	10.01(1)	10.16(1)	
$^1J(\text{P}_\text{B},\text{P}_\text{D})$	-187.04(8)	-181.54(2)	-177.38(1)	
$^2J(\text{P}_\text{B},\text{P}_\text{E})$	-92.75(8)	-99.47(3)	-107.58(1)	
$^2J(\text{P}_\text{C},\text{P}_\text{D})$	10.48(7)	10.06(2)	10.83(1)	
$^1J(\text{P}_\text{C},\text{P}_\text{E})$	-321.32(7)	-290.51(3)	-266.70(1)	
$^1J(\text{P}_\text{D},\text{P}_\text{E})$	-268.68(7)	-270.37(3)	-266.23(9)	
$^1J(\text{P}_\text{A},\text{W1})$			159	
$^1J(\text{P}_\text{A},\text{W2})$			144	
$^1J(\text{P}_\text{C},\text{W1})$			183	
$^1J(\text{P}_\text{C},\text{W2})$			132	
$^1J(\text{P}_\text{B},\text{W1})$			227	
$^1J(\text{P}_\text{D},\text{W2})$			170	
$^2J(\text{P}_\text{E},\text{W})$			20	

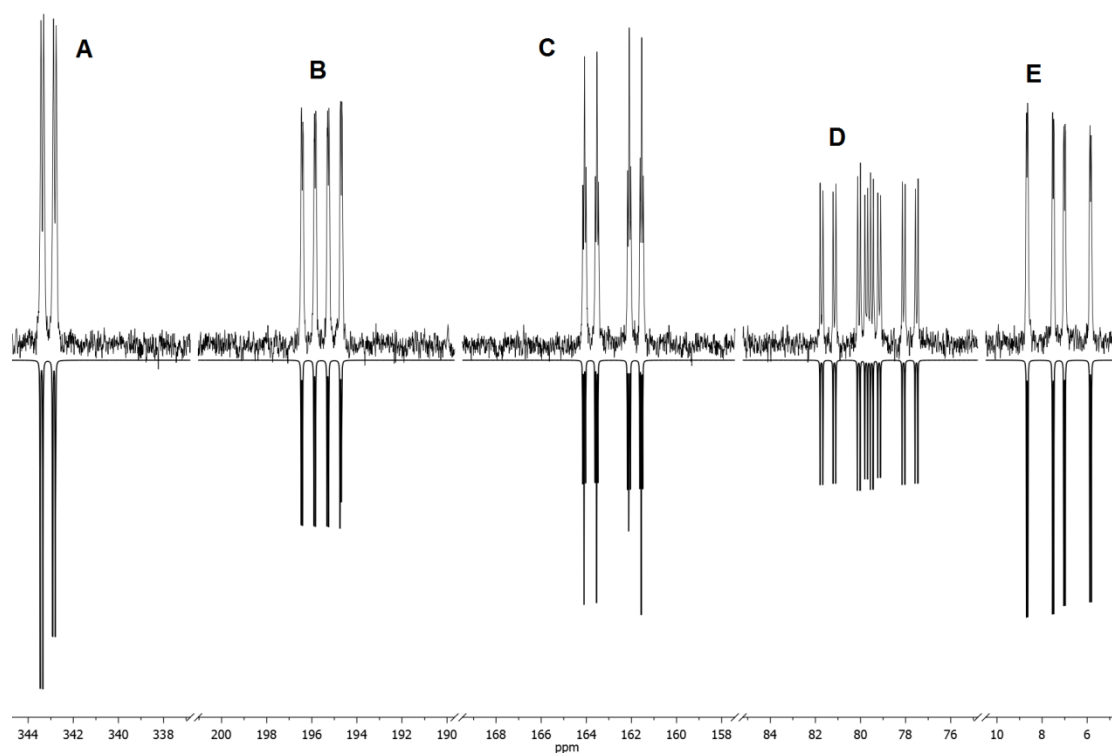


Figure S4. Experimental (top) and simulated (bottom) $^{31}\text{P}\{^1\text{H}\}$ NMR spectrum of complex **1a** in C_6D_6 .

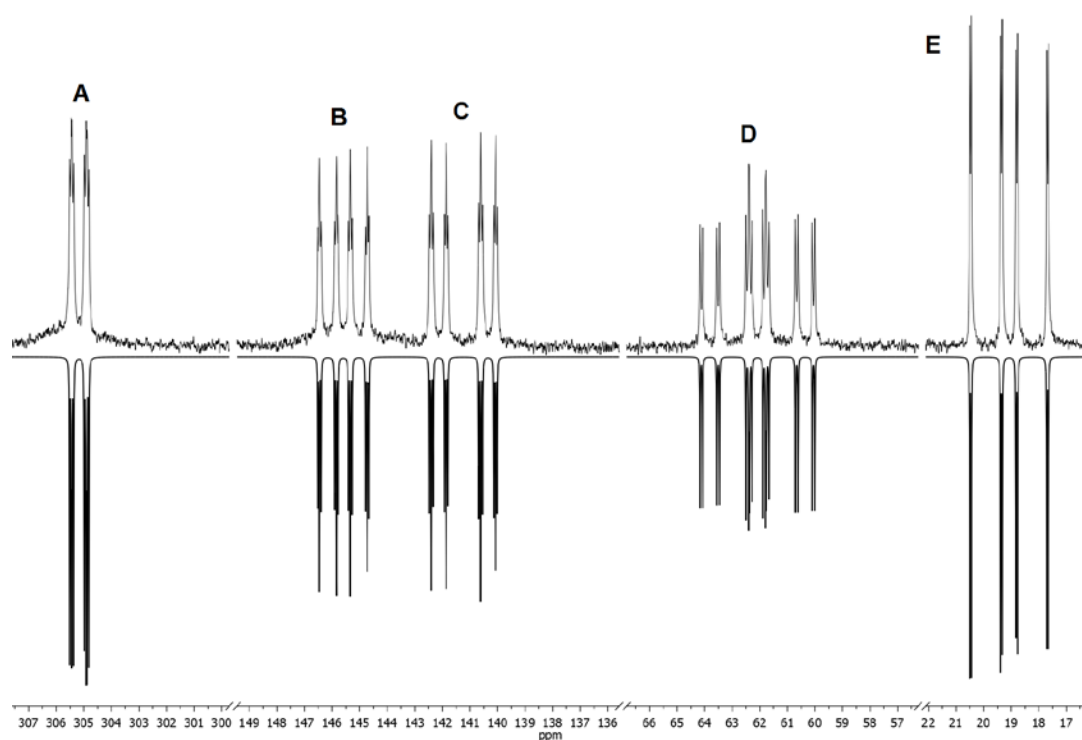


Figure S5. Experimental (top) and simulated (bottom) $^{31}\text{P}\{^1\text{H}\}$ NMR spectrum of complex **1b** in C_6D_6 .

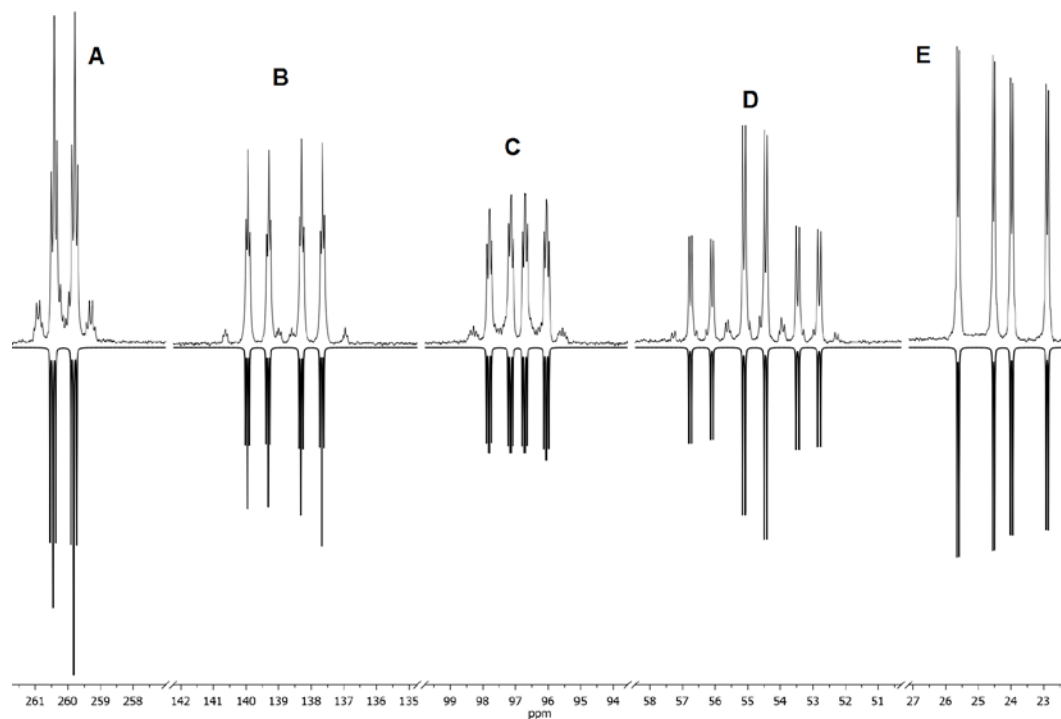


Figure S6. Experimental (top) and simulated (bottom) $^{31}\text{P}\{^1\text{H}\}$ NMR spectrum of complex **1c** in C_6D_6 .

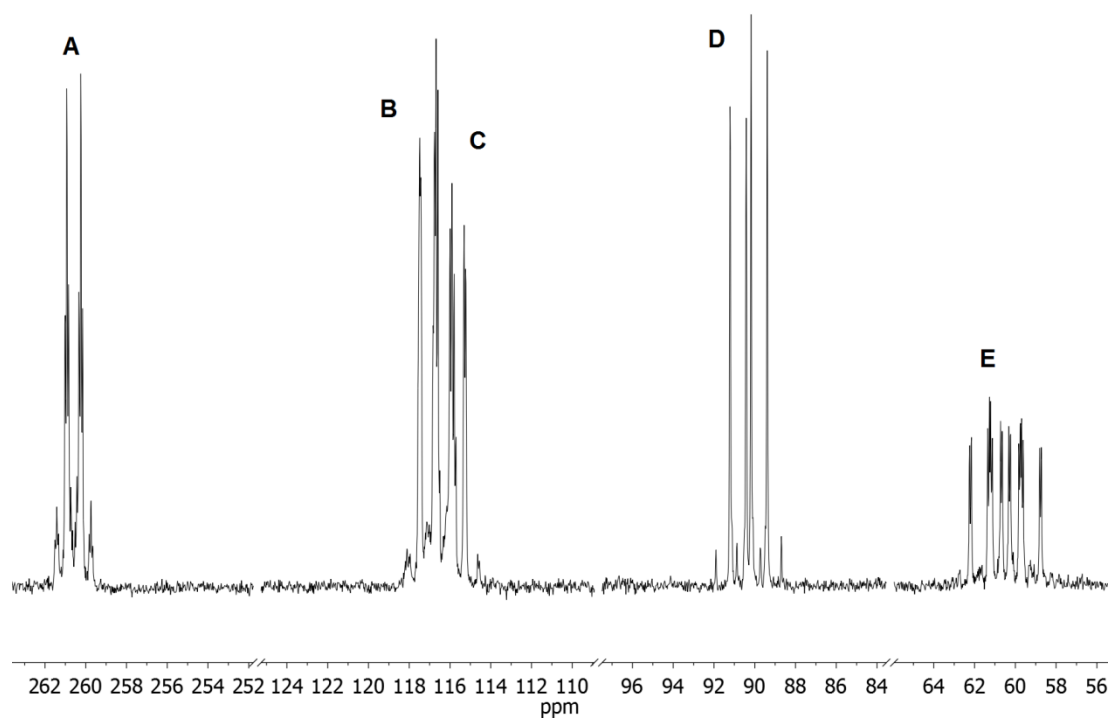


Figure S7. $^{31}\text{P}\{^1\text{H}\}$ NMR spectrum of complex **2c** in C_6D_6 .

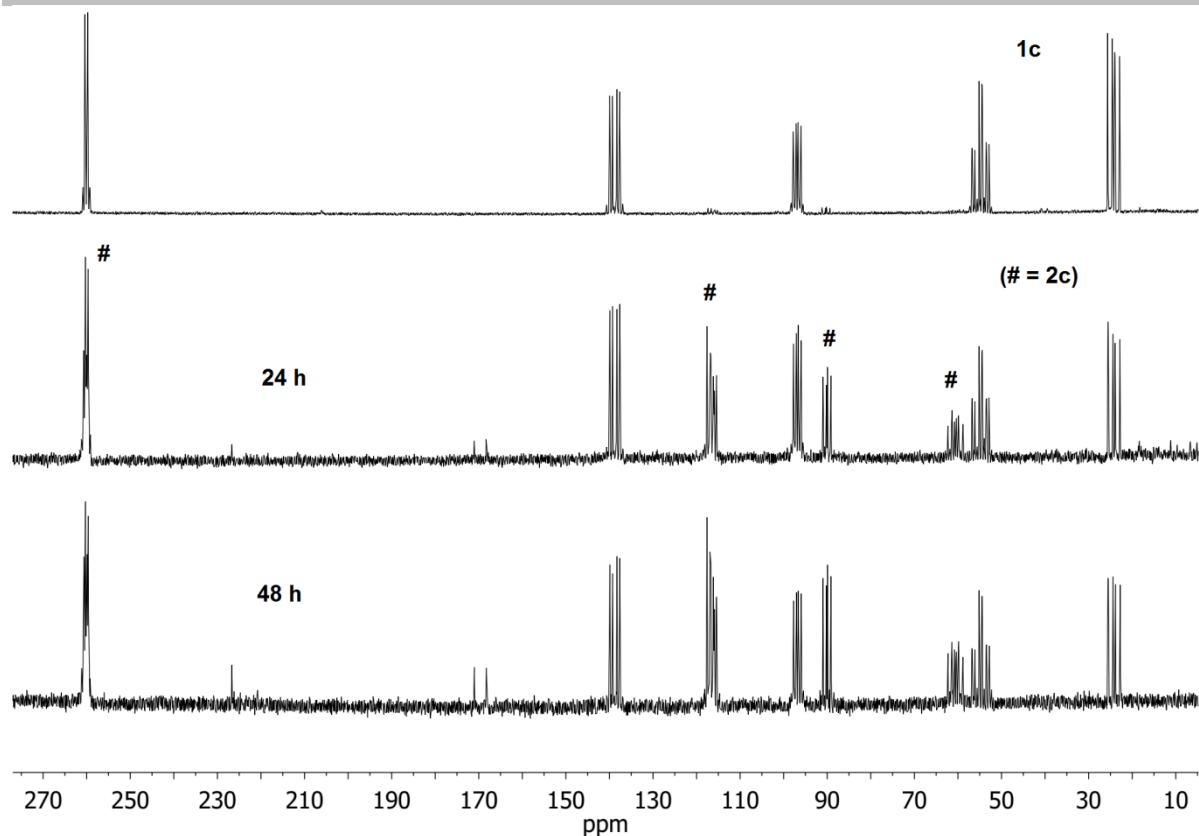


Figure S8. Time-dependent experimental $^{31}\text{P}\{^1\text{H}\}$ NMR spectra for the formation of complex **2c** compared to that of **1c** in C_6D_6 .

Table S4. CO and C=N vibrations (cm^{-1}) of compounds **1a–c** and **2c**.

Complex	$\nu(\text{CO})/\text{cm}^{-1}$					$\nu(\text{C=N})/\text{cm}^{-1}$
1a	1991s	1953vs	1938vs	1906s	1880sh	1635w
1b	2009s	1969vs	1954vs	1920s	1890sh	1634w
1c	2005s	1964vs	1947vs	1903s	1881sh	1629w
2c	2073s	2005s	1976vs	1940vs	1923vs	1632w

s = strong; sh = shoulder; vs = very strong; w = weak

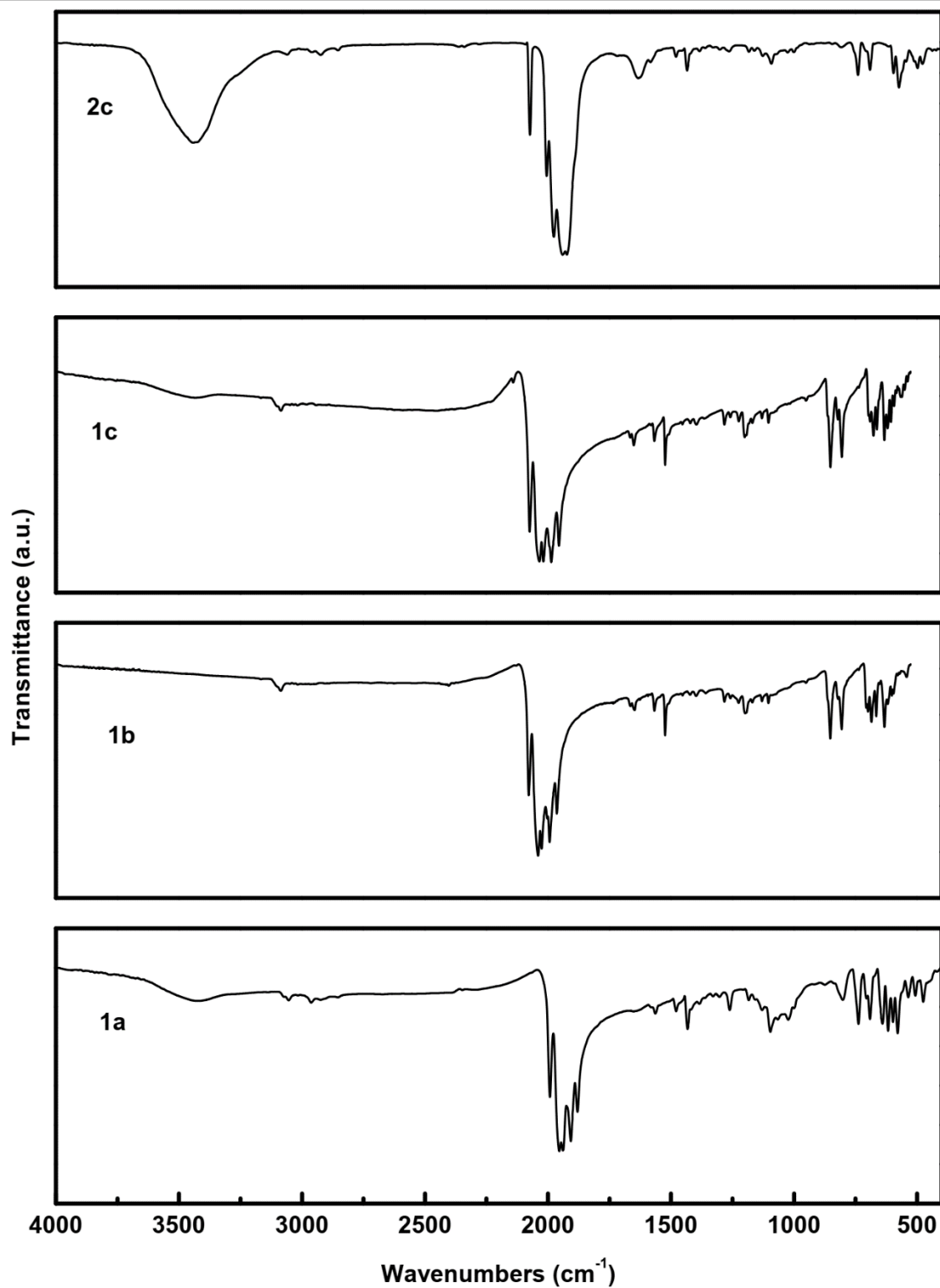


Figure S9. IR spectra of complexes compounds 1a–c and 2c.

The thermal properties of complexes 1b and 1c were studied by simultaneous TG/DTA/MS analyses in the temperature range 30–900 °C under an argon atmosphere (Fig. S10 and Table S5).

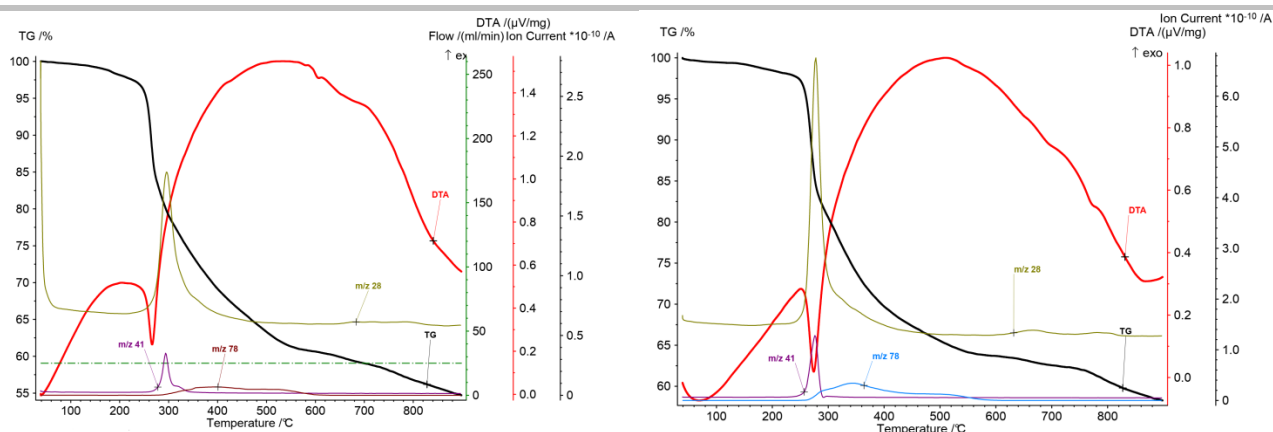


Figure S10. TG/DTA/MS plots for **1b** (left) and **1c** (right).

Table S5. Thermal decomposition data of **1b** and **1c** up to 900 °C.

Compound	Temperature Range (°)	Weight Loss (%)		Assignment
		Found	Calculated	
1b (M = 941.34)	200–290	21.53	22.20	6 CO + CH ₃ CN
	300–590	17.53	16.57	2 C ₆ H ₆
	600–900	6.23	6.59	2 P
1c (M = 1117.16)	170–290	18.34	18.71	6 CO + CH ₃ CN
	290–540	17.42	16.74	1 P + 3 C ₆ H ₆
	550–900	5.97	5.55	2 P

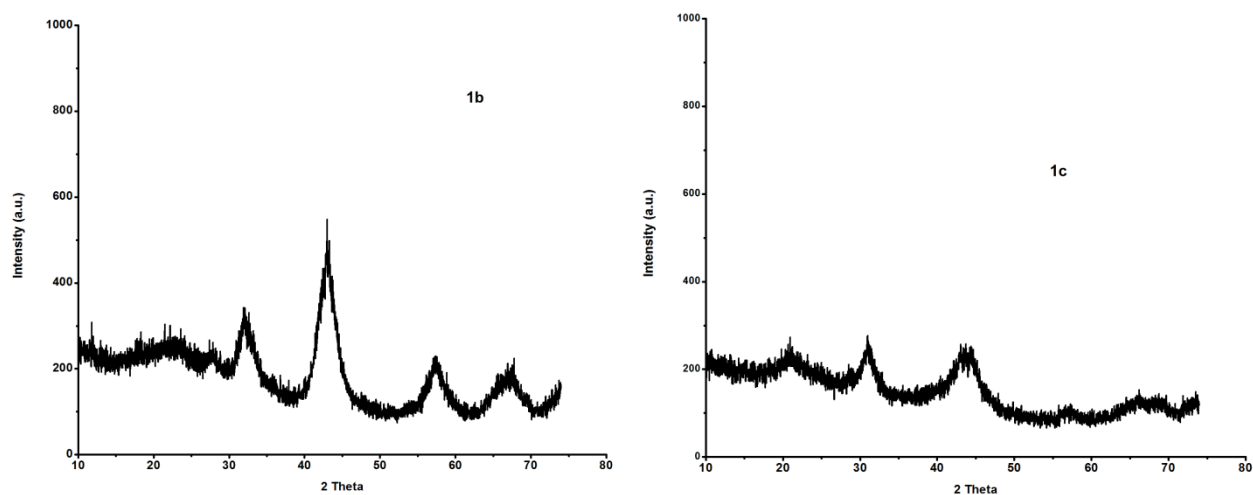


Figure S11. Powder XRD patterns of the thermal decomposition products of **1b** (left) and **1c** (right).

Powder XRD analyses were carried out on the residues of the samples from thermal decomposition. Measurements were performed with a STOE STADI-P powder diffractometer with a Cu-K α (1.540598 Å) X-ray source; tube power: 40 KV/40 mA; scan mode: Debye-Scherrer) using a borosilicate glass capillary as sample holder during the measurement. The powder diffraction patterns were analysed with the STOE powder diffraction system software in combination with the ICDD (International Centre for Diffraction Data) powder diffraction database. The PXRD patterns of the residues (Fig. S11) indicate that they are poorly crystalline, and the very low intensity peaks could not be indexed to any phase.

References

- [1] Kirk Marat, *SPINWORKS*, University of Manitoba Manitoba, Canada, **2010**.
- [2] J. J. Eisch, B. R. King, *Organometallic Syntheses. Transition-metal Compounds*, Academic Press, New York, London, **1965**.
- [3] D. P. Tate, W. R. Knipple, J. M. Augl, *Inorg. Chem.* **1962**, *1*, 433.
- [4] M. Scherer, D. Stein, F. Breher, J. Geier, H. Schoenberg, H. Gruetzmacher, *Z. Anorg. Allg. Chem.* **2005**, *631*, 2770.
- [5] D. M. Yufanyi, T. Grell, M.-B. Sárosi, P. Lönnecke, E. Hey-Hawkins, *Pure Appl. Chem.* **2019**, <https://doi.org/https://doi.org/10.1515/pac-2018-0905>.
- [6] *CrysAlis Pro: Empirical absorption correction*, Oxford Diffraction Ltd., **2014**.
- [7] A. Altomare, G. Cascarano, C. Giacovazzo, A. Guagliardi, M. C. Burla, G. Polidori, M. Camalli, *J Appl Crystallogr.* **1994**, *27*, 435.
- [8] a) G. M. Sheldrick, *Acta Crystallogr. Sect. C* **2015**, *71*, 3; b) G. M. Sheldrick, *Acta Crystallogr. Sect. A* **2015**, *71*, 3.
- [9] C. F. Macrae, P. R. Edgington, P. McCabe, E. Pidcock, G. P. Shields, R. Taylor, M. Towler, J. van de Streek, *J. Appl. Crystallogr.* **2006**, *39*, 453.
- [10] M. Basato, E. Brescacin, E. Tondello, G. Valle, *Inorg. Chim. Acta* **2001**, *323*, 147.